Amorphous defect clusters of pure Si and type inversion in Si detectors

E. Holmström and K. Nordlund

Department of Physics and Helsinki Institute of Physics, University of Helsinki, P.O. Box 64, Helsinki FIN 00014, Finland

M. Hakala

Department of Physics, University of Helsinki, P.O. Box 64, Helsinki FIN 00014, Finland

Si detectors subjected to energetic particle bombardment are known to undergo a deleterious type inversion from *n* type to *p* type. The effect is due to defects that trap electrons but the identity of the main responsible traps remains unknown. Using a combination of classical molecular-dynamics simulations and large-scale density-functional theory calculations, we show that amorphous defect clusters formed under particle bombardment are strong acceptors of electrons and may as such well explain the phenomenon.

I. INTRODUCTION

A heavily researched problem in materials physics is the effective type inversion of Si detectors as a consequence of energetic particle bombardment.[1–9] The effect is caused by lattice defects that form upon the interaction between incident energetic irradiation and the lattice atoms. The defects trap electrons and hence negative charge is accumulated into the *n*-type bulk of the detector. This eventually leads to the inversion of the sign of the space charge and an increase in the full depletion voltage of the device. Ultimately, this phenomenon destroys the functionality of the detector. The effect is a critically limiting factor for the lifetime of Si detectors in high luminosity colliders such as the Large Hadron Collider (LHC) and its prospective followers.[10–12]

Traditionally, the effort to identify the main responsible electron traps has focused on pointlike defects or impurities, such as vacancies and oxygen-related defects in crystalline Si.[1,3–7,11] However, that the same effect is observed in a wide range of different types of Si detectors with different impurity contents and doping concentrations suggests that a specific defect may not explain the type inversion under all circumstances. Instead, a more generic explanation independent of the type of Si should be sought. Recently, there has been an increasing emphasis on cluster-related defects, which are now believed to be responsible for the phenomenon.[12] More specifically, the search is on for cluster-related defects that are formed only after energetic hadron bombardment and whose behavior is independent of impurities. However, despite much research, the electron traps mainly responsible remain yet unidentified. In this study, we use classical molecular-dynamics (MD) simulations in conjunction with large-scale density functional theory calculations to show that amorphous defect clusters of pure Si, which are intrinsic defects generated by particle bombardment, act as strong acceptors of electrons and may as such explain the deleterious type inversion.

II. METHOD

The purpose of this study is to simulate the electronic structure of amorphous pockets or amorphous defect clusters that are formed as a result of energetic hadron bombardment in pure Si. It has been shown by previous simulations that collision cascades formed by already 5 keV recoils in Si are entirely broken down into small, isolated, liquidlike subcascades.[13] These subcascades then cool down rapidly to form amorphous pockets in the lattice. The existence of these inclusions has been confirmed experimentally[14–22] and their formation kinetics has been described by MD simulations.[13,23,24] Fully amorphous Si has been studied computationally to a great extent,[25–30] and much research has been done on isolated point defects in Si,[31] but amorphous clusters of defects surrounded by a crystalline lattice constitute a novel case that has not been studied with *ab initio* methods previously.

The simulation approach consisted of three parts. First, the ionic coordinates of the systems were created using classical MD simulations. The Si-Si interactions were modeled by the well-established Stillinger-Weber potential[32] and the computations were performed using the PARCAS MD code.[33] In the second part, the electronic structure of the resulting systems was determined using density-functional theory (DFT) pseudopotential plane-wave calculations within the local-density approximation (LDA) (Ref. 34) as parametrized by Perdew and Zunger.[35] These calculations were performed using the VASP code.[36] Finally, the average charge of the systems in the steady-state situation of a depleted Si detector bulk was determined using the results of Sah and Shockley,[37] which amounts to the extension of the well-known Shockley-Read-Hall statistics to multivalent defects.

DFT methods are prohibitively expensive for large numbers of atoms and initial testing showed that we could not afford to simulate systems larger than a few hundred Si atoms. Hence, instead of simulating full collision cascades using Si recoils in the lattice, we used the method of melting and quenching to emulate the experimental situation described above. This method has been shown to result in a structure similar to that obtained from full cascade simulations.[13] First, the center of a cubic crystalline simulation cell consisting of 512 Si atoms was melted by scaling the temperature of the center to 5000 K for a duration of 3 ps. Next, the cell was cooled down through the boundaries down to 0 K. Berendsen temperature control[38] was used throughout these initial simulations. 20 systems with an
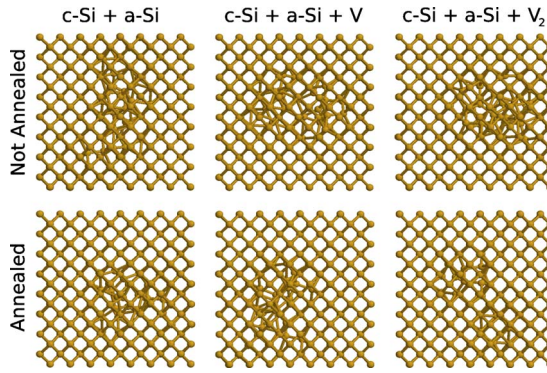
FIG. 1. (Color online) Example of the structure of a system in each of the six studied categories.

amorphous zone of ~10 Å in diameter and comprising ~50 defect atoms were created by this method. As defect clusters in Si are thought to be vacancy rich,[39,40] two variations were made to this scheme. In addition to the 20 created systems, two categories were added, one with an added vacancy (V) and another with an added divacancy (V_2) inside the amorphous zone. Finally, systems of each of these three categories were annealed by first keeping the cell at a temperature of 300 K for a period of 1 ns and then scaling the temperature of the cell to 0 K in a time of 10 ps. A relatively large amount of initial systems had to be created in order to produce 20 systems within the categories of annealed systems as well, as some 80% of the systems annealed out completely during the period of 1 ns, i.e., the crystalline state was fully recovered. The annealing was taken into account to better match the experimental situation of a Si detector at temperatures near 300 K. The result of these classical simulations was a total of 120 systems in six categories with an amorphous region in the center of the cell. An example of the structure of a system in each of the categories is presented in Fig. 1.

In the DFT part of the simulation scheme, the plane-wave cut-off energy and k-point sampling of the method were first tested for convergence. It was found that a cut-off energy of 200 eV and a $4 \times 4 \times 4$ Monkhorst-Pack[41] grid of k points produced highly converged total energies and densities of states for the system of 512 atoms. Due to computational limitations, no further structural relaxation except for test calculations was performed within the DFT scheme. For the same reason we limited our calculations to the defect charge states +, 0, and −. The positions of the (0/−) and (+/0) ionization levels for each of the 120 systems were determined from formation energy differences according to the usual practice.[42,43] Additionally, the levels were determined from the highest energy value in the total density of occupied states within charge states 0 and − of each system. Finally, the average charge of the systems, assuming a depleted Si bulk in a steady-state condition at a temperature of 300 K, was computed using the results of Sah and Shockley.

It is necessary to assess the performance and reliability of the hybrid simulation scheme described above, regarding the structures, ionization levels, and the final average charge state of the systems. This is particularly important because of the well-known limitations of LDA DFT in describing band gaps of semiconductors. For the structures, we first investi-

gated the monovacancy in the crystal, which is a well-understood system. The structure given by the Stillinger-Weber potential showed a relative volume change of −55% for the tetrahedron formed by the four nearest-neighbor ions of the vacancy. This is qualitatively correct as compared to the result of −40% obtained by high-precision conjugate-gradient relaxation within LDA for the neutral vacancy by Puska *et al.*[44] According to them, the charge states + and − also have a similar volume change. In addition to the mono-vacancy, we studied a randomly chosen system from each of the six categories introduced above. Using full conjugate-gradient relaxation until the maximum force acting on any atom was 0.3 eV/Å, we found that changes in the relaxed structures in relation to the unrelaxed ones were generally small. The mean displacement of any atom was at the most 0.3 Å in each of the studied systems and the maximum atomic displacement for a given system was generally well below 1.0 Å.

The ionization levels obtained within our hybrid method can be investigated against previous experimental and DFT studies of the monovacancy and the divacancy in crystalline Si in order to draw conclusions about their typical offset with respect to experimentally determined values. Specifically, the aim is to understand how the computed level (0/−) would compare with experiment, as the position of this and subsequent negative levels are critical in driving the type inversion. For the monovacancy, the ionization levels related to the charge states 2+, +, and 0 are located in the lower part of the gap, below $E_v + 0.15$ eV. Since no ionic relaxation is included, this is reasonably close to previous DFT calculations[44] (levels below $E_v + 0.19$ eV) and experiments[31] (levels mostly below $E_v + 0.13$ eV). The ionization levels related to the charge states 0, −, and 2−, are on the other hand, underestimated. In our case they are below $E_v + 0.37$ eV while experimentally they are around midgap ($E_v + 0.56$ eV) or in the upper part of the gap.[31] In the case of the divacancy, our levels related to the charge states +, 0, −, and 2− are all below $E_v + 0.26$ eV, which tend to underestimate the experimental levels [e.g., (−/2−) at $E_v + 0.75$ eV (Ref. 45)]. However, fully relaxed, spin-polarized LDA calculations by Pesola *et al.*[46] also underestimate the level (−/2−), placing it at $E_v + 0.43$ eV.

The above results for crystalline Si show that the position of the level (0/−) for V or V_2 is underestimated maximally by 0.4 eV compared to the real crystal. There is no experimental comparison data for our novel case of amorphous pockets in Si but we believe that the value of 0.4 eV is a good conservative estimate for the discrepancy (i.e., underestimation) between our calculations and the experimental situation in the case of amorphous pockets. In particular, we will use this upper limit to check the correctness of our qualitative conclusions.

Finally the (+/0) and (0/−) levels for one randomly chosen amorphous system in each of the six categories were calculated with and without DFT relaxation in the +, 0, and − charge states. It was verified that changes in the positions of the levels after DFT relaxation were generally small. Test calculations were also performed within the generalized gradient approximation using the Perdew-Wang 91 functional (PW91).[47] Differences to the LDA calculations proved negligible.

TABLE I. Average position of the first donor $(+/0)$ and acceptor level $(0/-)$ with respect to the valence-band maximum, as determined from differences in total energies (ΔE_f) and from the density of states (ϵ). A and B refer to nonannealed and annealed systems, respectively. The error estimate is the standard deviation. All values are in eV.

	$(+/0)$				$(0/-)$			
	ΔE_f		ϵ		ΔE_f		ϵ	
Composition	A	B	A	B	A	B	A	B
c-Si+a-Si	0.17 ± 0.03	0.15 ± 0.04	0.18 ± 0.03	0.18 ± 0.05	0.23 ± 0.04	0.25 ± 0.04	0.26 ± 0.04	0.29 ± 0.04
c-Si+a-Si+V	0.14 ± 0.05	0.14 ± 0.04	0.16 ± 0.05	0.16 ± 0.04	0.22 ± 0.05	0.22 ± 0.04	0.25 ± 0.05	0.27 ± 0.04
c-Si+a-Si+V_2	0.14 ± 0.05	0.13 ± 0.04	0.15 ± 0.05	0.15 ± 0.05	0.20 ± 0.04	0.23 ± 0.06	0.23 ± 0.04	0.27 ± 0.06

III. RESULTS AND DISCUSSION

The average position of the first donor and acceptor level for each category of studied systems is presented in Table I. It can be seen that the states are located in the lower half of the experimental band gap of 1.12 eV, relatively close to the valence-band maximum. Also, there are practically no differences between the nonannealed and annealed systems. The positions of the states as derived from the density of states for each system are slightly higher but within error margins with respect to the results from total-energy differences. The distribution of the positions of the states within the band gap is visualized in Fig. 2. In the figure the annealed and nonannealed systems, yielding very similar defect levels, were summed together for simplicity. It is seen here that there are no notable differences in the position distributions of the states between different compositions of the systems. Strikingly, it can be particularly observed that having an extra vacancy or divacancy in the amorphous cluster has practically no effect on the level positions.

The first acceptor levels of three sample systems are visualized in Fig. 3. The isosurface of the electron density of the orbital is shown at 50% and 10% of the maximum electron density for each case. It can be seen that in all systems the state encompasses practically the whole of the amorphous region without preference to any particular atomic, interstitial, or vacancy site, and there is some spread of the state into the surrounding region. The amorphous defect cluster thus looks to offer a spectrum of states where electrons can be trapped and the localization of these states is determined by the extent of the amorphous region. In other words, the electronic levels of these amorphous clusters cannot be described in terms of a group of individual point-defect levels, but rather such a cluster acts as a single, multivalent defect in the lattice. We believe that this qualitative result can be generalized to other materials as well but the positions of the levels in the gap are naturally dependent on the material in question.

The fact that the levels are located well below midgap implies immediately that in a steady-state situation, such as in a depleted Si detector bulk, the average charge in the defect will be negative. This is shown quantitatively by the charge state analysis, which predicts an average charge of -1.0 for the studied set of systems. The effect of higher acceptor levels would possibly be an even more negative average charge than unity. In order to gain further confidence in this conclusion, the charge state analysis was repeated after shifting all the calculated $(0/-)$ levels up by 0.4 eV, based on the considerations of Sec. II. Even in this case, one still obtains a negative average charge of -0.1 for the entire set of systems.

Thus we have found that amorphous defect clusters are strong candidates for driving the type inversion of Si detectors under particle bombardment. In the experimental setup, this type of cluster-related defect would be formed only after energetic hadron bombardment, which, alongside the independence from impurities, fulfills the known properties of the sought-after electron trap mainly responsible for the type inversion. The observation that intrinsic defect clusters can explain the *n*-type to *p*-type inversion indeed offers a natural explanation for the fact that the same type inversion is observed in a wide variety of detectors. A future calculation should also include the effect of the electric field which is applied over the detector for depletion, and a more precise treatment of the quantum mechanical exchange and correla-
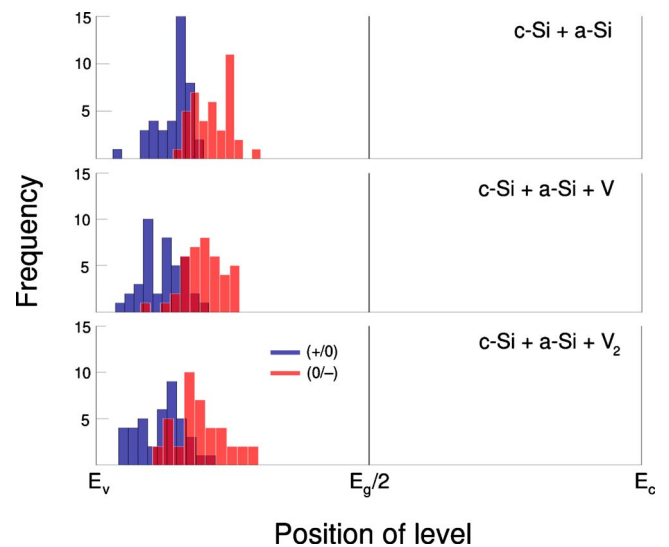
FIG. 2. (Color online) Distribution of the first donor and acceptor levels within the experimental band gap of Si as calculated from total-energy differences. Here both the annealed and nonannealed systems were considered as a single category for each composition, resulting in 40 systems for each of the three categories shown. The midgap position is marked by the vertical line. E_v and E_c signify the top of the valence band and the bottom of the conduction band, respectively.
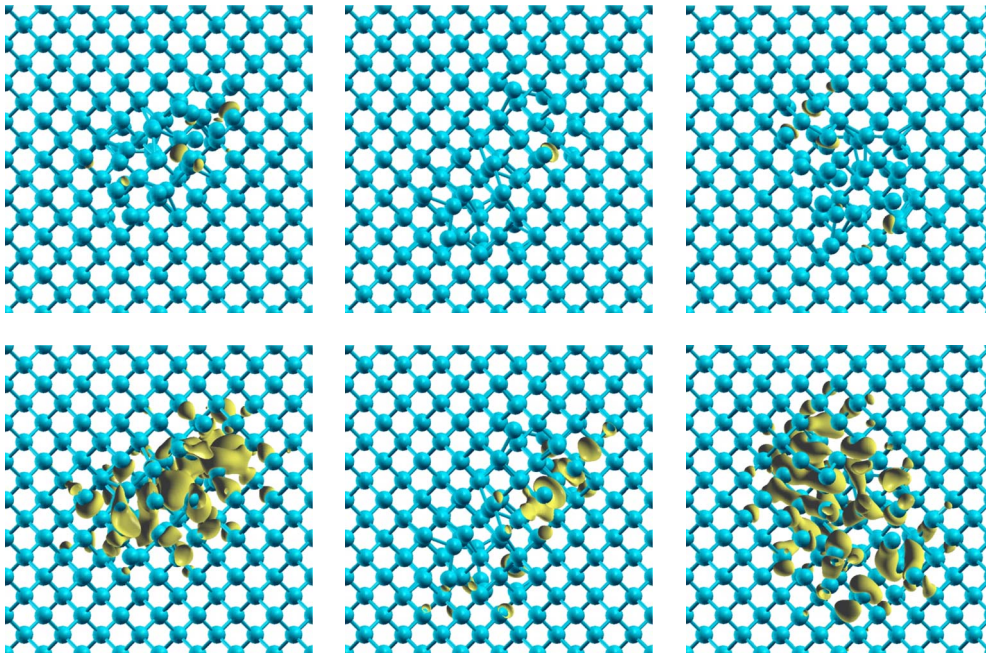
FIG. 3. (Color online) Visualizations (Ref. 48) of the isosurface of the electron density of the first acceptor state of three sample systems at 50% (upper row) and 10% (lower row) of the maximum electron density of the orbital. The first column represents an a-Si+c-Si system, the second column an annealed a-Si+c-Si+V system, and the third column shows an a-Si+c-Si+V_2 system.

tion would allow for the refinement of the energy-level positions. Further calculations are needed to complete the characterization of the multivalent nature of these amorphous pockets. Determining all the levels within the gap would give an estimate of the possible effect of these amorphous defect clusters on leakage current, as this effect is dominated by states in the midgap region.

IV. CONCLUSIONS

In conclusion, large-scale density-functional theory calculations in conjunction with classical molecular-dynamics simulations were performed to study the electronic structure of amorphous defect clusters embedded in pure crystalline Si. It was found that these defects are powerful electron traps. As it is believed that the traps mainly responsible for the effective type inversion of Si detectors are cluster-related defects which are independent of impurities, amorphous defect clusters thus constitute a strong candidate for the defects responsible for the deleterious effect.

[1] B. C. MacEvoy, G. Hall, and K. Gill, Nucl. Instrum. Methods Phys. Res. A **374**, 12 (1996).

[2] RD2 Collaboration, G. N. Taylor, F. Fares, S. J. Bates, C. Furetta, M. Glaser, F. Lemeilleur, E. Leon-Florian, C. Gößling, B. Kaiser, A. Rolf, R. Wunstorf, H. Feick, E. Fretwurst, G. Lindström, M. Moll, and A. Chilingarov, Nucl. Instrum. Methods Phys. Res. A **383**, 144 (1996).

[3] K. Gill, G. Hall, and B. MacEvoy, J. Appl. Phys. **82**, 126 (1997).

[4] M. Huhtinen, Nucl. Instrum. Methods Phys. Res. A **491**, 194 (2002).

[5] I. Pintilie, E. Fretwurst, G. Lindström, and J. Stahl, Appl. Phys. Lett. **82**, 2169 (2003).

[6] J. Harkonen *et al.*, Nucl. Instrum. Methods Phys. Res. A **541**, 202 (2005).

[7] I. Pintilie, M. Buda, E. Fretwurst, G. Lindström, and J. Stahl, Nucl. Instrum. Methods Phys. Res. A **556**, 197 (2006).

[8] A. G. Bates and M. Moll, Nucl. Instrum. Methods Phys. Res. A **555**, 113 (2005).

[9] N. Manna, D. Bassignana, M. Boscardin, L. Borrello, M. Bruzzi, D. Creanza, M. de Palma, V. Eremin, A. Macchiolo, D. Menichelli, A. Messineo, V. Radicci, M. Scaringella, and E. Verbiskaya, Nucl. Instrum. Methods Phys. Res. A **583**, 87 (2007).

[10] V. Eremin, E. Verbitskaya, and Z. Li, Nucl. Instrum. Methods Phys. Res. A **476**, 537 (2002).

[11] CERN RD50 Collaboration Status Report 2002/2003, 2003, http://rd50.web.cern.ch/RD50/

[12] CERN RD50 Collaboration Status Report 2007, 2007, http://rd50.web.cern.ch/RD50/

[13] T. Diaz de la Rubia and G. H. Gilmer, Phys. Rev. Lett. **74**, 2507 (1995).

[14] T. E. Gessner, M. Pasemann, and B. Schmidt, Phys. Status Solidi A **77**, 133 (1983).

[15] M. O. Ruault, J. Chaumont, J. M. Penisson, and A. Bourret, Philos. Mag. A **50**, 667 (1984).

[16] O. W. Holland, C. W. White, M. K. El-Ghor, and J. D. Budai, J. Appl. Phys. **68**, 2081 (1990).

[17] M. Alurralde, F. Paschoud, M. Victoria, and D. Gavillet, Nucl. Instrum. Methods Phys. Res. B **80-81**, 523 (1993).

[18] S. U. Campisano, S. Coffa, V. Raineri, F. Priolo, and E. Rimini, Nucl. Instrum. Methods Phys. Res. B **80-81**, 514 (1993).

[19] J. S. Williams, R. D. Goldberg, M. Petravic, and Z. Rao, Nucl. Instrum. Methods Phys. Res. B **84**, 199 (1994).

[20] S. E. Donnelly, R. C. Birtcher, V. M. Vishnyakov, and G. Carter, Appl. Phys. Lett. **82**, 1860 (2003).

[21] P. Partyka, Y. Zhong, K. Nordlund, R. S. Averback, I. M. Robinson, and P. Ehrhart, Phys. Rev. B **64**, 235207 (2001).

[22] R. J. Schreutelkamp, J. S. Custer, J. R. Liefting, W. X. Lu, and F. W. Saris, Mater. Sci. Rep. **6**, 275 (1991).

[23] K. Nordlund, M. Ghaly, R. S. Averback, M. Caturla, T. Diaz de la Rubia, and J. Tarus, Phys. Rev. B **57**, 7556 (1998).

[24] M.-J. Caturla, T. Diaz de la Rubia, L. A. Marques, and G. H. Gilmer, Phys. Rev. B **54**, 16683 (1996).

[25] R. Car and M. Parrinello, Phys. Rev. Lett. **60**, 204 (1988).

[26] I. Štich, R. Car, and M. Parrinello, Phys. Rev. B **44**, 11092 (1991).

[27] I.-H. Lee and K. J. Chang, Phys. Rev. B **50**, 18083 (1994).

[28] M. Durandurdu, D. A. Drabold, and N. Mousseau, Phys. Rev. B **62**, 15307 (2000).

[29] S. Hara, S. Izumi, T. Kumagai, and S. Sakai, Surf. Sci. **585**, 17 (2005).

[30] A. Valladares, R. Valladares, F. Alvarez-Ramirez, and A. A. Valladares, J. Non-Cryst. Solids **352**, 1032 (2006).

[31] For a review, see E. G. Seebauer and M. C. Kratzer, Mater. Sci. Eng. R. **55**, 57 (2006).

[32] F. H. Stillinger and T. A. Weber, Phys. Rev. B **31**, 5262 (1985).

[33] K. Nordlund, 2006, PARCAS computer code. The main principles of the molecular-dynamics algorithms are presented in Refs. 23 and 49. The adaptive time step and electronic stopping algorithms are the same as in Ref. 50.

[34] For a review, see R. O. Jones and O. Gunnarsson, Rev. Mod. Phys. **61**, 689 (1989).

[35] J. P. Perdew and A. Zunger, Phys. Rev. B **23**, 5048 (1981).

[36] G. Kresse and J. Hafner, Phys. Rev. B **47**, 558 (1993); **49**, 14251 (1994); G. Kresse and J. Furthmüller, Comput. Mater. Sci. **6**, 15 (1996); Phys. Rev. B **54**, 11169 (1996).

[37] C.-T. Sah and W. Shockley, Phys. Rev. **109**, 1103 (1958).

[38] H. J. C. Berendsen, J. P. M. Postma, W. F. van Gunsteren, A. DiNola, and J. R. Haak, J. Chem. Phys. **81**, 3684 (1984).

[39] Y. Shi, D. X. Shen, F. M. Wu, and K. J. Cheng, J. Appl. Phys. **67**, 1116 (1990).

[40] R. M. Fleming, C. H. Seager, D. V. Lang, P. J. Cooper, E. Bielejec, and J. M. Campbell, J. Appl. Phys. **102**, 043711 (2007).

[41] H. J. Monkhorst and J. D. Pack, Phys. Rev. B **13**, 5188 (1976).

[42] S. B. Zhang and J. E. Northrup, Phys. Rev. Lett. **67**, 2339 (1991).

[43] A. Höglund, O. Eriksson, C. W. M. Castleton, and S. Mirbt, Phys. Rev. Lett. **100**, 105501 (2008).

[44] M. J. Puska, S. Poykko, M. Pesola, and R. M. Nieminen, Phys. Rev. B **58**, 1318 (1998).

[45] G. D. Watkins and J. W. Corbett, Phys. Rev. **138**, A543 (1965).

[46] M. Pesola, J. von Boehm, S. Poykko, and R. M. Nieminen, Phys. Rev. B **58**, 1106 (1998).

[47] J. P. Perdew, J. A. Chevary, S. H. Vosko, K. A. Jackson, M. R. Pederson, D. J. Singh, and C. Fiolhais, Phys. Rev. B **46**, 6671 (1992).

[48] A. Kokalj, J. Mol. Graphics Modell. **17**, 176 (1999).

[49] M. Ghaly, K. Nordlund, and R. S. Averback, Philos. Mag. A **79**, 795 (1999).

[50] K. Nordlund, Comput. Mater. Sci. **3**, 448 (1995).